Journal of Polymer Research (2020) 27: 162
https://doi.org/10.1007/s10965-020-02132-2

ORIGINAL PAPER

Investigation of long-term ageing effect on the thermal properties of chicken feather fibre/poly(lactic acid) biocomposites

Tarkan Akderya[1] · Uğur Özmen[2] · Buket Okutan Baba[3]

Received: 7 December 2019 / Accepted: 22 April 2020 / Published online: 18 May 2020

Abstract

In this study, the effects of long-term natural atmospheric ageing on the thermal properties of chicken feather fibre reinforced poly(lactic acid) biocomposite materials having chicken feather fibre mass content of 2, 5, and 10% were investigated. Chicken feather fibres, which are bio-based reinforcement material, and poly(lactic acid), which is bio-based matrix material, are compounded with a twin-screw extruder and injection-moulded; hence, the biocomposite material is produced. The effect of long-term natural atmospheric ageing on the thermal stability, crystallization, and melting behaviour of the biocomposite materials were analysed by thermogravimetric, derivative thermogravimetry, differential thermal, and differential scanning calorimetry analyses. In addition, the fracture surface of the samples was examined in depth by scanning electron microscopy analysis. The experimental results show that the long-term natural ageing process decreases the thermal stability values of the biocomposite materials and increases the glass transition temperatures and degree of crystallinities.

Keywords Chicken feather fibre · Poly(lactic acid) · Biocomposites · Thermal properties · Ageing

Introduction

Some unique features of fibre-reinforced polymer-based composite materials discovered in the past decades have led to a shift in research, engineering, and industry interest from monolithic materials to fibre-reinforced polymer-based composites [1, 2]. Some of these unique features are high strength/weight ratio, high chemical resistance, non-corrosive properties, good insulating properties, and high fracture toughness. These composite materials consist of high strength fibres such as glass or carbon and low strength polymeric matrix, but they do not have renewability, recyclability, and biodegradability properties. In addition to that, they carry health risks if inhaled. Although fibre-reinforced polymeric composites have been widely used over the years in the aerospace, entertainment, automotive, construction, and sports industries to provide solutions to many structural problems due to their low cost and moderate strength advantages, the use of these materials may cause a serious environmental problem in the following years [2–6].

The consumer's developing sensitivity to consider the environmental impact at all stages of the life cycle, including processes such as final disposal and recycling, and sanctions on environmental legislation increase the pressure on material manufacturers. Due to the increased environmental awareness on a worldwide scale, there has been an increasing trend of interest in the production of recyclable and environmentally sustainable composite materials [7–10]. The use of new generation biocomposite materials consisting of natural fibres and biodegradable matrix as substitutes for glass or carbon fibre reinforced polymer composites can help eliminating the environmental problems mentioned above; therefore, it can provide better living conditions [11, 12].

Biocomposite materials, which are partly eco-friendly or green composites, are classified according to their structure of the fibres and the matrix. The components of green composites are derived from renewable sources; hence, green composite materials reduce the dependence on petroleum-

✉ Tarkan Akderya
takderya@gmail.com

[1] Department of Biomedical Engineering, Faculty of Engineering and Architecture, University of Bakırçay, Menemen, 35660 Izmir, Turkey

[2] Department of Mechanical Engineering, Faculty of Engineering, Manisa Celal Bayar University, Muradiye, 45140 Manisa, Turkey

[3] Department of Mechanical Engineering, Faculty of Engineering and Architecture, Izmir Katip Çelebi University, Çiğli, 35620 Izmir, Turkey

based fibre and matrix. Partly eco-friendly composites can be formed by two different methods. The first is made up of a combination of man-made or synthetic fibres with a biopolymer matrix. The other is formed by the combination of natural fibres and a petroleum-based non-degradable matrix [5, 13–15].

Poly(lactic acid) (PLA) is a significant biopolymer that is recyclable and completely degradable after its service life. The production process of the PLA begins with the transformation of starch derived from starch-rich crops such as corn. It is followed by the process of effective preparation of lactic, and finally, it ends with the polymerization of lactic. In terms of a life cycle, the use of biopolymeric matrix PLA has been found to reduce greenhouse gas emissions by up to 40% and also to reduce non-renewable energy use by up to 25% compared to petrochemical-based polymers like as polyethylene or polyethylene terephthalate [16–22].

Natural fibres have distinct superior properties such as availability, low density, low cost (on a volumetric basis), flexibility during processing, highly specific stiffness, high acoustic attenuation, low carbon footprint, low production energy consumption, and biodegradability compared to synthetic fibres [23–25]. Natural fibres can be classified in three different ways: animal, plant, and mineral based [23]. Examples of natural plant-based fibres include ramie [26], kenaf [27], abaca [28], banana [29], sisal [30], cotton [31], kapok [32], wheat [33], bamboo [34], corn [35], loofah [36], soya [37], poplar [38], pineapple [39], henequen [40], flax [41], hemp [42], jute [43], coir [44], oil palm [45], rice husk [46], and totora [47]. Mineral-based natural fibres include amosite [48], crocidolite [49], actinolite [50], chrysotile [51], tremolite [52], and anthophyllite [50]. Some natural animal-based fibres are horsehair [53], human hair [54], alpaca hair [55], sheep wool [56], and chicken feather [57].

Animal-based natural fibres such as chicken feather fibres (CFF), have recently attracted great attention in engineering industries and innovative product design. Therefore, the use of CFF as a reinforcement for polymer-based biodegradable materials has slowly increased. Because of its superior characteristic properties such as recyclability and renewability, the CFF has been recognized as a new reinforcement element for polymer-based composites [2, 57–59]. One of the studies in which CFF is used as reinforcement in polymeric materials was done by Bessa et al. [60]. In the study, thermal and acoustic insulation properties of a composite material formed by using thermoset epoxy resin reinforced by CFF were investigated. According to thermal resistance and acoustic insulation test results, CFF has high potential to be used as reinforcements in composite materials. Bessa et al. [60] has also found that the thermal resistance of CFF/epoxy composite materials is positively dependent on the mass fraction of CFF (80:20, respectively, CFF and epoxy). Another study was conducted by Zhan et al. [61], and in this study, the electrical resistances of CFF/epoxy and E-glass/epoxy composite materials were investigated. The electrical resistance of CFF/epoxy composites has been found to be greater than that of E-glass/epoxy composites. One of the studies investigating the properties of biocomposite material, which was produced by the use of PLA as matrix and CFF as reinforcement, was conducted by Özmen et al. [62]. In this study, the change of thermal characteristic properties of CFF/PLA was investigated, and according to thermogravimetric analysis (TGA) results, it was found that CFF/PLA biocomposite material has higher thermal stability than pure PLA. In another study, Cheng et al. [63] investigated the thermal and mechanical properties of CFF/PLA biocomposite materials and found that the addition of CFF enhances the thermal stability of the green composites compared to pure PLA.

In order to determine the long-term durability of a new product such as a biocomposite and guarantee its reliability of use under certain conditions, it is important to understand the ageing process of the product. Studies on the ageing of biocomposites can support existing knowledge and help to promote their use in real-life applications. Accelerated ageing studies carried out under the conditions of artificial environment, which are prepared to investigate the effects of temperature or different parameters, are aimed to obtain faster results [64, 65]. Isadounene et al. [66] identified changes in physico-mechanical properties by accelerated ageing of PLA biocomposites reinforced with alkali-treated olive husk flour. The results show that when the ageing process was prolonged, the mechanical properties of the biocomposite reduced as a result of the plasticization of PLA and the swelling effect. Lila et al. [67] studied the accelerated thermal ageing behaviour of PLA based biocomposites reinforced with bagasse fibres. According to the results obtained from X-ray diffraction and dynamic mechanical analysis, they concluded that a significant change in crystallinity and glassy transition behaviour occurred during the ageing period. Gil-Castell et al. [68] investigated the effect of accelerated hydrothermal ageing on the thermal stability and morphological properties of sisal/PLA biocomposites. The results showed that the increased crystallinity decreases thermal stability values. Under long-term service conditions, polymeric materials are known to exhibit susceptibility to degradation, and they are subjected to thermal, photochemical, oxidative or even hydrolytic degradation, either individually or simultaneously [69, 70]. In this context, it is necessary to determine the performance of polymer-based composites under real service conditions for use in specialized applications [71]. Le Duigou et al. [72] subjected the injection-moulded flax/PLA biocomposites to natural seawater long-term ageing for two years and determined the changes in their properties. After the immersion, breakage of the fibres and reduced ability to bond between PLA and the fibres were observed.

Under atmospheric conditions, PLA slowly degrades, and the degradation process may last for 3–5 years. Due to the inherent complex morphology of polymeric composite materials, it is difficult to estimate their performance under service conditions. The parameters used in the production process, such as the production temperature and the production method, affect the thermomechanical properties of the composites; thus, the composites can exhibit anisotropic and non-linear behaviour under service conditions [73, 74]. Long-term ageing under room conditions has serious effects on the performance of composite materials, and it can alter the physical properties of the amorphous phase of glassy polymers [75]. Prolonged ageing of PLA-based biocomposites under room conditions has an important role in determining the shelf-life of these materials, and no studies have been reported in this area.

It can be seen from the literature review, there are very few studies investigating the properties of CFF-reinforced composites, and in addition, no research has yet been made on how long-term atmospheric ageing affects the properties of the biocomposites. In general, studies on ageing are accelerated under artificial conditions due to time constraints. While it is possible to obtain useful information on the long-term performance of biocomposites from accelerated ageing studies, there is a great need for real-time studies. Because only in this way, it will be possible to determine the shelf life of composites and how long they can work under real service conditions. The aim of this study is to find out how the thermal properties of biocomposite materials produced by adding different amounts of CFF to PLA thermoplastic matrices are affected by long-term atmospheric environmental ageing condition. The thermal properties of pure PLA and CFF/PLA biocomposite samples were already determined before the ageing process, and after the ageing process applied, the thermal properties were examined with the same thermal characterisation test equipment and parameters. In this context, mass loss-temperature curves by applying TGA, derivative mass loss-temperature curves by applying derivative thermogravimetry (DTG) analysis, decomposition temperatures by overlapping TGA-differential thermal analysis (DTA) curves, some characteristic temperatures such as glass transition (*Tg*), enthalpy, and crystallinity values by applying differential scanning calorimetry (DSC) analysis were determined for both aged and non-aged samples. Furthermore, the analysis was deepened by the addition of scanning electron microscopy (SEM) micrographs of the fracture surfaces. CFF/PLA biocomposites produced with variable CFF composition ratios, long-term ageing duration, controlled experimental environment, and material design are critical outputs of this study. The data obtained from this long-term ageing study under real-time exposure allow us to compare the data obtained as a result of accelerated ageing studies which are carried out under the conditions of artificial environment.

Experimental procedures

Material production, specimen preparation, and long-term ageing conditions

Prior to the production process of the biocomposite material, white CFF, which were supplied in a raw condition from a local company in Manisa/Turkey, were subjected to several preparation processes. The raw fibres were in the range of 20–40 μm in diameter and about 20 mm in length. Rachises of the CF were manually cut into barbs to obtain CFF from them. A detailed illustration of a typical white chicken feather is given in Fig. 1.

In order to determine the effect of the CFF mass content on the thermal properties of the biocomposites, CFF mass ratios of 2, 5, and 10% were used. The WiseStir HT-50AX mixer was used to mix PLA with CFF at predetermined mass ratios. CFF/PLA biocomposite materials were produced by injection moulding with the aid of a twin-screw extruder at a speed of 150 rpm and a final extruder temperature of 205 °C. The biocomposite material variables used in this study are shown schematically in Fig. 2. In addition, detailed information on CFF/PLA biocomposite material production processes can be found in the study of Özmen et al. [62] and Baba et al. [76].

Environmental atmospheric long-term ageing of biocomposite materials was carried out by storing specimens in a special container for 5 years (43,800 h) in a laboratory environment at a temperature of 23 ± 2 °C and average humidity of 50 ± 5%. Laboratory temperature and humidification were provided by air conditioning during the ageing process in order to avoid unstable conditions. Samples were kept under ideal living conditions without being affected by direct sunlight and airflow. Production procedure of this study is illustrated in Fig. 3.

Characterisation methods

Thermal characterisation

TGA, DTG, DTA, and DSC thermal characterisation tests were performed to determine how the ageing process affects the thermal stability and thermal properties of CFF, pure PLA, and CFF/PLA biocomposite material. TGA, DTG, DTA tests were performed by heating the samples having a mass of 10–20 mg from 30 to 500 °C using a TA TGASDT Q600 thermal analysis instrument under a nitrogen atmosphere of 50 ml/min at a heating rate of 10 °C/min. In order to determine $_{Tg}$ values, crystallization, and melting characteristics of pure PLA and CFF/PLA samples, DSC analysis technique was used. DSC analyses of both aged and non-aged samples were performed with DSC-TA Q10 instrument at a temperature increasing rate of 10 °C per minute from 28 to 300 °C.

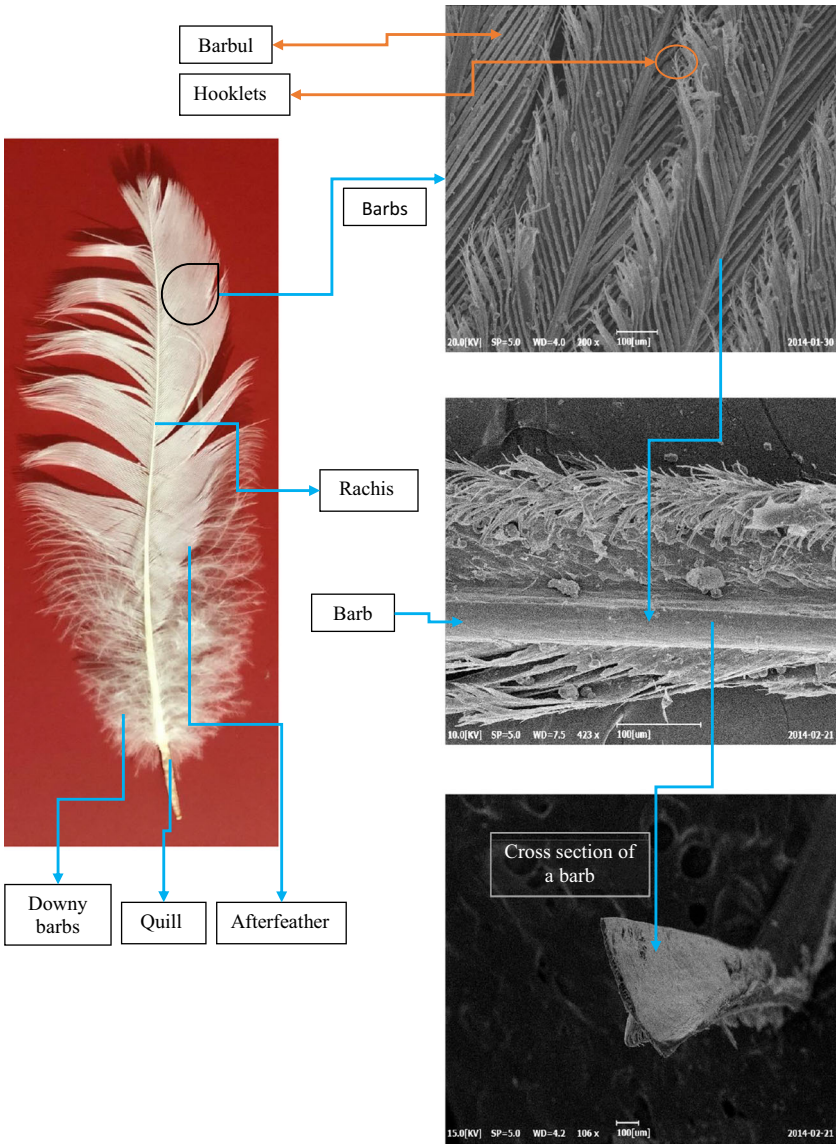

Fig. 1 The detailed view of a chicken feather

Morphological characterisation

SEM analysis was carried out to analyse the fracture surface morphology of the PLA and CFF/PLA samples. In order to achieve micrographs from the fracture surface of the non-aged CFF/PLA composites, a COX EM-30 SEM device with an acceleration voltage of 15 kV in accordance with the E986 standard was used. Field Emission Scanning Electron Microscope Carl Zeiss 300VP was used with the same parameters to investigate the fracture surfaces of aged samples.

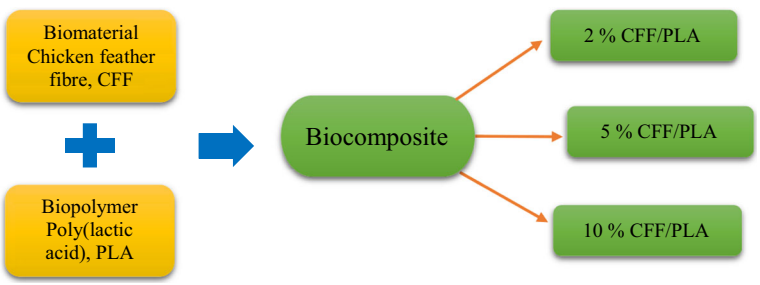

Fig. 2 The components of CFF/PLA biocomposite material

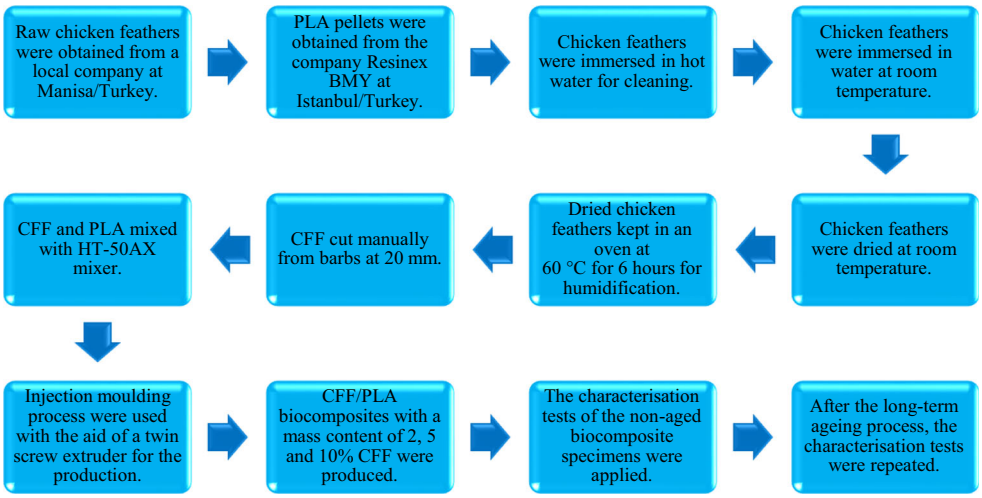

Fig. 3 Detailed production procedure

Results and discussion

TGA, DTG, DTA, DSC, and SEM analyses were performed to determine how thermal properties of CFF/PLA biocomposite material, which is composed of PLA matrix and CFF fibre reinforcement in mass ratios of 2, 5, and 10%, are affected by long-term ageing (43,800 h) process.

Thermogravimetric, derivative thermogravimetry, and differential thermal analyses

The thermal decomposition of non-aged and long-term aged CFF/PLA biocomposites is shown in TGA curves presented in Fig. 4. The mass loss of non-aged and aged PLA, CFF, and CFF/PLA biocomposite samples occurs in three steps [63, 77, 78]. In the first mass loss step, it is noticed that the volatile content and moisture in the sample evaporate by the effect of increasing temperature [63, 77, 79]. It is clear from the thermographs that the percentage of volatile content relative to the total mass is quite low. In the second mass loss step, pure CFF, pure PLA, and CFF/PLA biocomposite samples begin to degrade. In the third step, the material starts to decompose. It is observed that the mass losses due to decomposition increase continuously as the temperature increases, and the most serious mass losses occur at this step. The mass loss at this step means that the thermal stability is reduced due to the decomposition of the material [80, 81].

Among the non-aged samples (Fig. 4 (a)), PLA has the highest total mass loss, while CFF has the lowest mass loss. Three mass loss steps for the CFF are consecutive to eliminate the adsorbed water, destruction of disulphide bonds (cystine) arising from amino acid in the keratin structure and evaporation of hydrogen sulfide, and moderate decomposition of keratin structure in CFF [82]. PLA shows a decomposition of 99.46% from the initial testing temperature of 30 °C to the end testing the temperature of 500 °C. The mass losses of non-aged CFF/PLA biocomposites decrease with the increasing mass content of CFF in the biocomposite, as evidenced by the TGA curves in Fig. 4 (a).

According to the TGA curves of the aged samples in Fig. 4 (b), the order of mass losses of the aged samples is the same as that of the non-aged ones (Fig. 4 (a)). The highest mass loss belongs to PLA with 99.37%, and the lowest mass loss belongs to CFF with 71.25%. When the mass losses of the non-aged samples and the aged ones are compared with each other, it is seen that the long-term ageing process does not affect the mass loss of PLA, but it increases the mass losses of CFF/PLA biocomposites and reduces that of CFF.

The total mass losses are higher for the aged biocomposites compared to the non-aged ones. CFF/PLA biocomposites are thermally stable until 250 °C, and above 250 °C, they begin to decompose due to the presence of CFF. Since the mass of the samples remains unchanged around 400 °C, PLA matrices are decomposed, and the remaining residue results from CFF. Due to the higher amount of keratin, the composites with higher CFF content start degrading at lower temperatures than the composites with lower CFF content [77] for both non-aged and aged samples.

Figure 5 shows derivative mass-temperature graphs of the non-aged and long-term aged samples, and it points out the temperature at which the highest decomposition rate of the CFF, PLA, and CFF/PLA biocomposite samples with the same CFF content. The decomposition temperature is indicative of materials resistance to temperature, and it can be affected by factors such as thermal ageing process [83, 84]. For the case of non-aged samples, the highest decomposition peak belongs to PLA samples with 357.70 °C, and the lowest decomposition peak belongs to CFF with 329.79 °C. It is observed that decomposition temperatures of 2, 5, and 10% CFF/PLA samples decrease with the increasing CFF content. Similarly, the aged sample with the highest decomposition temperature is PLA (348.03 °C), and the lowest one is CFF (326.53 °C). Although the decrease in decomposition temperatures due to ageing effect is more pronounced in PLA than in CFF, it can be commented that the

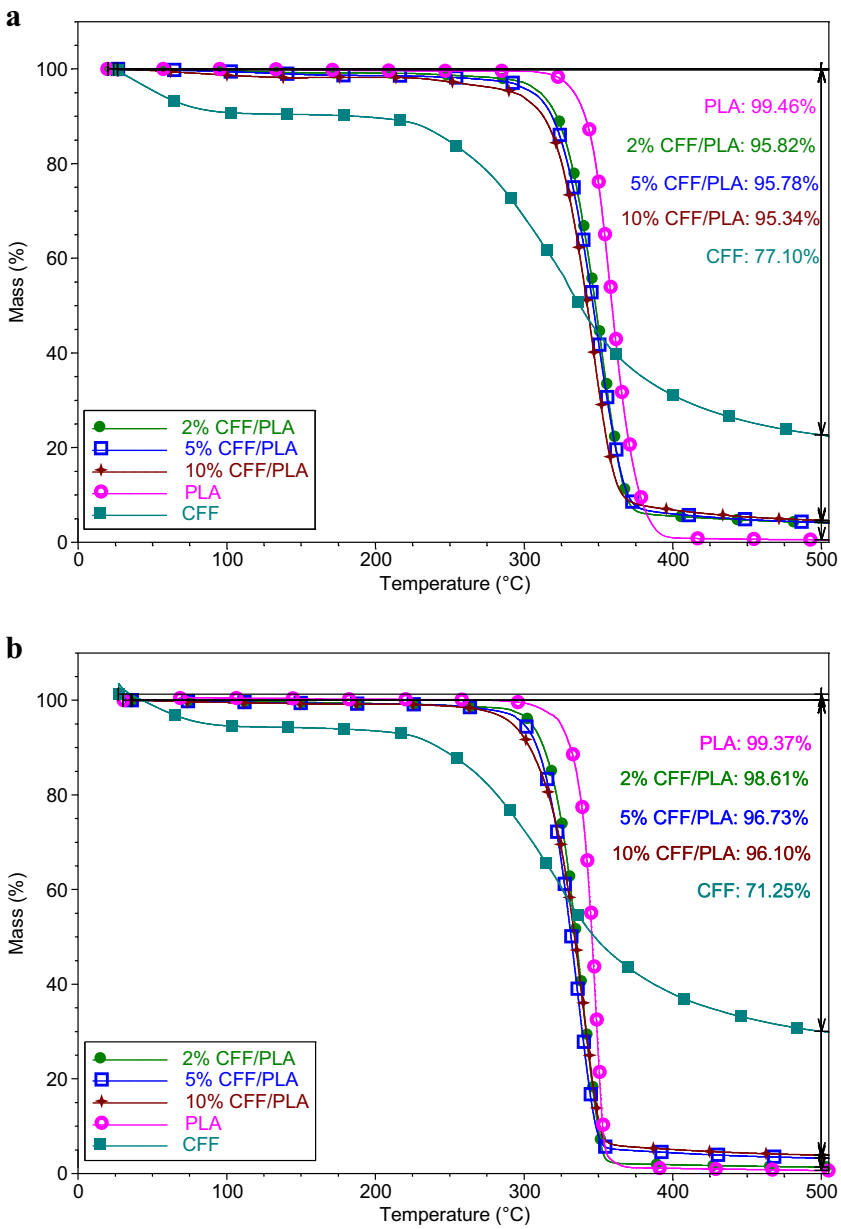

Fig. 4 TGA curves of (**a**) non-aged and (**b**) aged samples

ageing process reduces the decomposition temperatures of all the samples.

By overlapping the DTA and the TGA thermographs, the peak (T_{peak}), onset (T_{onset}), and endset (T_{enset}) temperatures on the DTA curve corresponding to the TGA curve as mass loss values can be found (Fig. 6). As a representative example, the mass loss steps of aged 2% CFF/PLA biocomposite samples are detailed in Fig. 6. The first two steps correspond to a lower mass compared to the third mass loss phase, which can be called the complex area on the DTA thermograph includes two endothermic peaks and a complex peak. Since this area includes the T_{onset}, the temperature at which the decomposition begins, the thermal stability of the composite can be determined with T_{onset} [85–87]. 1.97% of the mass is lost by evaporation of adsorbed water from hydrophilic groups of CFF, and 10.33% mass is lost by the degradation of the composite between steps two and three corresponding to 290.58 (T_{2i}) to 315.30 (T_{onset}) °C, respectively. In step three, T_{onset}, at which the material begins to decompose, is also accepted as the thermal stability, and this value is 315.30 °C. The material experiences the most serious decomposition rate at 344.44 °C, and the complex area ends at 364.71 °C. In the complex area, 2% CFF/PLA biocomposite loses 85.54% of the sample mass. Composite materials can be used up to high temperatures without degradation due to their good thermal properties such as thermal stability. These temperatures correspond to the onset temperature of the material [81, 86, 88].

Critical values obtained from TGA-DTA curves of the all samples are given in Table 1. As can be seen from Table 1, T_{onset} of the non-aged 2% CFF/PLA biocomposite sample is

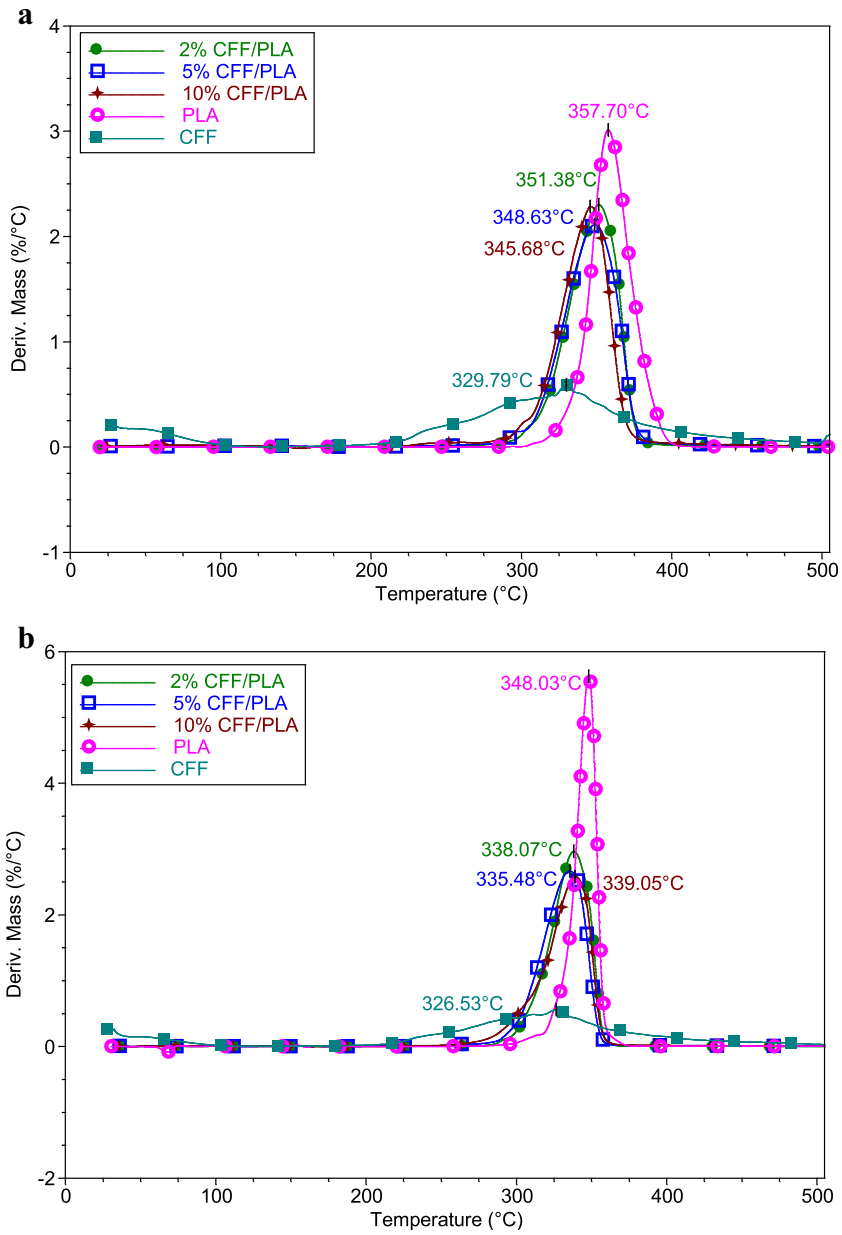

Fig. 5 DTG curves of **(a)** non-aged and **(b)** aged samples

319.60 °C, while this temperature dropped to 315.30 °C with the effect of long-term ageing. The aged 5% CFF/PLA sample has less volatile content (3.04% vs. 3.24%), while the percentage of content degraded in step two (6.64% vs. 4.97%) and the percentage of content decomposed within the complex area increase (85.19% vs. 84.56%). In addition to this, with the effect of ageing process, greater mass loss occurs in the aged 5% CFF/PLA sample (%96.73 vs. %95.78). The thermal stability of the 10% CFF/PLA biocomposite sample decreases with the effect of ageing. T_{onset} of the non-aged sample is 316.10 °C, while T_{onset} of the aged one is 315.66 °C. When the volatile content percentages are evaluated, non-aged 10% CFF/PLA sample has greater content with 4.67%. The content of the aged 10% CFF/PLA sample that degraded in step two is higher with 17.41%. The total mass loss of the aged 10% CFF/PLA sample is higher than that of the non-aged one (96.10% vs. 95.34%). When Table 1 is examined for PLA, it is observed that aged PLA has less volatile content, and the start temperature of second step (T_{2i}), which is the starting point of the degradation, decreases sharply from 326.43 to 304.64 °C. The thermal stability of the PLA sample also decreases from 338.41 °C to 336.43 °C with the effect of ageing. When the percentages of PLA sample decomposed within the complex area is examined, they are 91.41% and 80.59% for the aged and the non-aged, respectively. In addition, when the total mass loss of PLA is evaluated, it is seen that the mass losses of the non-aged and aged sample are almost the same. The thermal stability value of the CFF decreases with the effect of

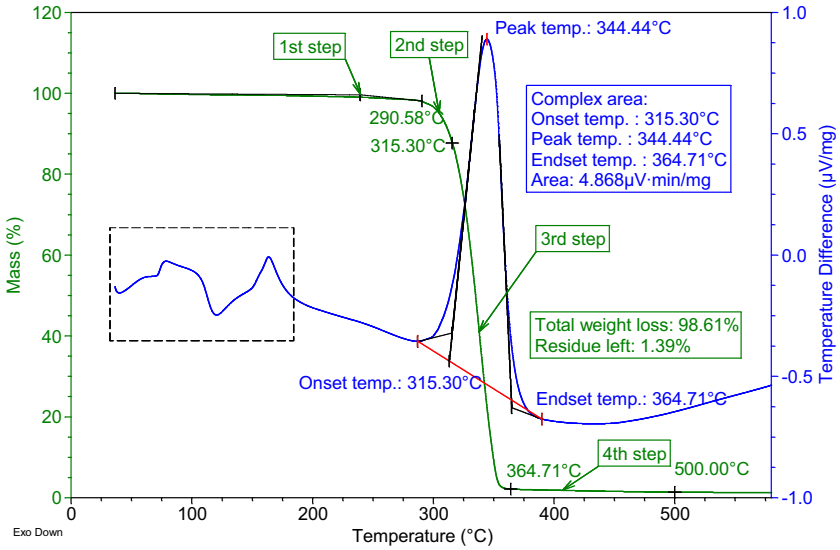

Fig. 6 TGA – DTA curve of the aged 2% CFF/PLA biocomposite sample

ageing (232.75 °C vs. 231.57 °C). The volatile content of the non-aged CFF appears to have a greater percentage by mass (9.10% vs. 6.48%), while the percentage of aged CFF decomposed within the complex area appears to be greater (14.04% vs. 30.99%). Taking the entire table into consideration, it is noticed that the non-aged samples contain more volatile content. It is obvious that T_{onset}, which indicate the thermal stability in all samples, and T_{2i} are seen to decrease with the effect of long-term ageing in all samples. Under the influence of ageing process, T_{onset} ,T_{2i}, and volatile contents decrease, while the total mass loss in both CFF and CFF/PLA biocomposite samples increases.

In this study, the degradation rate, which means the decomposition of the material with the effect of temperature, is obtained by summing up the mass losses of material occurring in the 2nd and 3rd (complex area) steps. The degradation rates of all samples are given in Fig. 7. Accordingly, when the aged and non-aged of the CFF, PLA, and CFF / PLA biocomposites

Table 1 Degradation and decomposition temperatures of PLA, CFF, and CFF/PLA biocomposites

Sample	1st step	2nd step		Complex area (3rd step)					% mass loss in 4th step	% Total mass loss
	% mass loss	T_{2i} °C	% mass loss	T_{onset} °C	T_{endset} °C	T_{peak} °C	Area µV.min/mg	% mass loss		
Non-aged 2% CFF/PLA	2.89	299.80	5.71	319.60	376.71	354.27	5.37	84.97	2.25	95.82
Aged 2% CFF/PLA	1.97	290.58	10.33	315.30	364.71	344.44	4.87	85.54	0.77	98.61
Non-aged 5% CFF/PLA	3.24	294.55	4.97	315.69	377.53	352.22	5.80	84.56	3.01	95.78
Aged 5% CFF/PLA	3.04	291.33	6.64	308.40	361.18	340.96	4.05	85.19	1.86	96.73
Non-aged 10% CFF/PLA	4.67	290.12	7.34	316.10	370.46	348.90	4.75	79.21	4.12	95.34
Aged 10% CFF/PLA	1.77	266.72	17.41	315.66	362.32	343.70	3.59	74.84	2.08	96.10
Non-aged PLA	2.18	326.43	5.51	338.41	404.79	368.69	13.10	91.41	0.36	99.46
Aged PLA	0.92	304.64	16.93	336.43	366.48	352.05	6.39	80.59	0.93	99.37
Non-aged CFF	9.10	203.27	2.07	232.75	290.22	243.85	1.04	14.04	51.89	77.10
Aged CFF	6.48	201.36	1.76	231.57	324.64	243.75	9.33	30.99	32.02	71.25

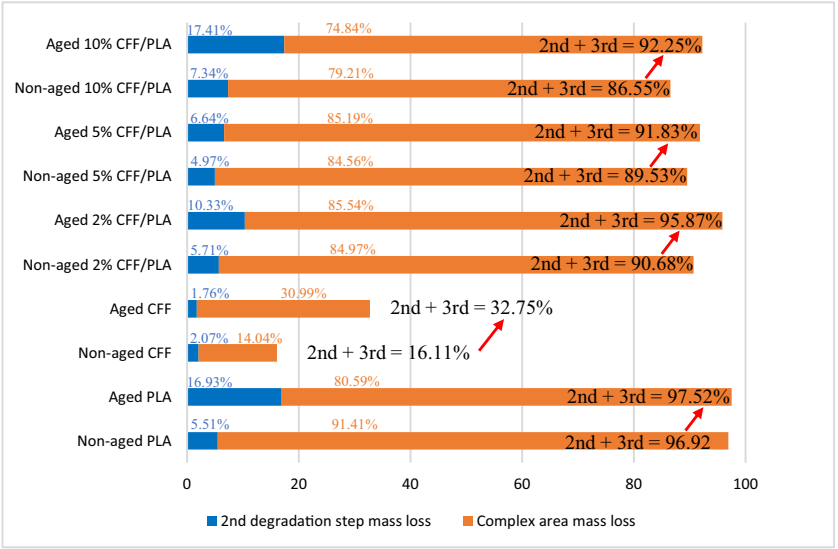

Fig. 7 Degradation rates of the samples according to TGA-DTA curves

are evaluated among themselves, an increase in the degradation rates is observed in all samples with the effect of the ageing process. At the same time, the degradation rates of the samples, whose thermal stability decreases with the effect of ageing, increase.

Differential scanning calorimetry analyses

DSC thermograms are recorded to observe the effects of the long-term ageing process on the crystallization and melting behaviour of PLA and CFF/PLA biocomposite samples. Figure 8 illustrates the DSC curves of the samples while Table 2 shows the DSC parameters of the non-aged and aged PLA and CFF/PLA biocomposite samples. In general, DSC measures the flow of heat during an endothermic or exothermic process that develops in a controlled environment due to time and temperature function. In the DSC plot, the upper transition peaks indicate the heat requiring endothermic zone, while the down transition peaks reveal heat-releasing exothermic zone. T_g and decomposition temperatures (T_m) are obtained from the endothermic transition peaks, while the crystallization temperature (T_c) is obtained from the exothermic peak. In addition, cold-crystallization enthalpy (ΔH_c) and melting enthalpy (ΔH_m) can be obtained from DSC graphs while the degree of crystallization (X_c) can be calculated by the following Eq. (1) [89]:

$$X_c = \frac{\Delta H_m - \Delta H_c}{w \Delta H_m^0} \times 100\% \quad (1)$$

w represents the mass fraction of PLA, and the melting enthalpy of all crystalline PLA (ΔH_m^0) is taken as 93 J/g in the literature [62, 87, 90].

The DSC thermogram generated for non-aged PLA and CFF/PLA biocomposites is presented in Fig. 8 (a). All exothermic and endothermic peaks are clearly visible in Fig. 8. Accordingly, the first endothermic peak between 57.65–62.85 °C indicates the T_g. PLA has the highest T_g with 62.85 °C, the T_g of 2% CFF/PLA is 58.65 °C, the T_g of 5% CFF/PLA is 57.65 °C, and the T_g of 10% CFF/PLA is 60.45 °C. All CFF/PLA biocomposite samples have lower T_g values than pure PLA. As can be seen in the graph, the T_g of the 10% CFF/PLA biocomposite sample, which has the highest CFF mass, is greater than the 2% and 5% CFF/PLA samples. The reason for the lack of a trend may result not only from the non-homogeneous mixture of PLA at higher concentration of CFF (10%) but also from the heterogeneity of the different parts of the CFF [64]. Exothermic transition peaks between 106.35 °C and 124.85 °C refer to the crystallization temperatures. The highest T_c belongs to PLA with 124.85 °C, and the lowest T_c belongs to 5% CFF/PLA biocomposite sample with 106.35 °C. Considering the energies released during crystallization, the amount of energy released increases with the increasing CFF content. The lowest ΔH_c belongs to PLA with 2.89 J/g, while the highest ΔH_c belongs to 10% CFF/PLA biocomposite sample with 23.20 J/g. Declines in the ΔH_m and X_c values of non-aged samples are observed with the increasing CFF content. The ΔH_m value for pure PLA is 30.10 J/g, while it is 25.31 J/g for the 10% CFF/PLA biocomposite sample, resulting in a loss of 15.91%.

The thermogram with DSC curves of aged pure PLA and CFF/PLA biocomposite samples is given in Fig. 8 (b). According to this thermogram, the T_g values ranged from 66.80 °C to 67.96 °C, so it can be stated that there is no significant change. When T_c values are considered, the highest T_c belongs to PLA with 117.10 °C, whereas for biocomposite samples these values range from 108.75 °C to 109.78 °C. The ΔH_c value of PLA is 25.18 J/g. The ΔH_c value is 20.84, 25.25

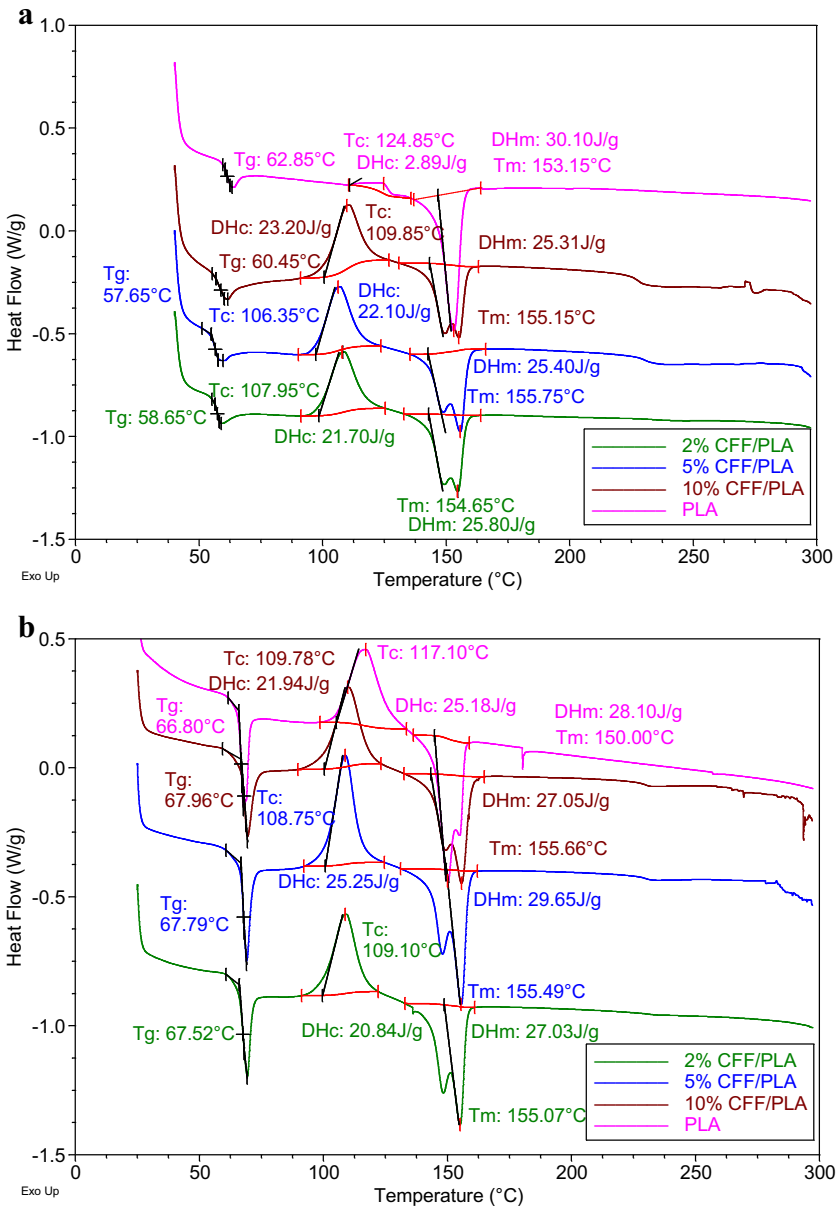

Fig. 8 DSC curves of (**a**) non-aged and (**b**) aged samples

and 21.94 J/g for 2, 5, and 10% CFF/PLA biocomposites, respectively. When T_m values are taken into consideration, values of CFF/PLA biocomposites are higher than pure PLA. As CFF content increases, T_m value increases. The lowest T_c belongs to PLA with 150.00 °C, while the highest T_c value belongs to 10% CFF/PLA with 155.66 °C. In addition, the highest ΔH_m value belongs to 5% CFF/PLA biocomposite samples with 29.65 J/g.

T_g refers to the temperature region where the polymer changes from a rigid, glassy structure to a soft, rubbery structure. The T_g value can be affected by parameters such as ageing, thermal applications, polymer architecture, and degree of crystallinity [91, 92]. Ageing mechanism and ageing products can cause a change in the molecular chain structure of PLA [91]. According to Table 2, it is observed that all T_g values of aged samples increase compared to those of the non-aged samples with the same CFF mass content. This increase in T_g is attributed to the steric hindrance effect in biocomposite samples. This finding suggests that ageing mechanism may inhibit the mobility of the chains, possibly due to recrystallization phenomena occurred in the long-term ageing period [35, 84, 93].

When the ΔH_m and $X_c$values of CFF/PLA biocomposites are compared, it is observed that these values are higher in the aged ones. This finding may be explained by the phenomenon of lamella thickening. The phenomenon of lamella thickening results from chain scissions of CFF/PLA biocomposite sample chains during the long-term ageing process. Chain scission results in the formation of shorter molecules with higher mobility. These modified chains recrystallize during the long-

Table 2 DSC results of non-aged and aged PLA - CFF/PLA biocomposites

Sample	T_g (°C)	T_c (°C)	ΔH_c (J/g)	T_m (°C)	ΔH_m (J/g)	X_c (%)
Non-aged PLA	62.85	124.85	2.89	153.15	30.10	29.26
Aged PLA	66.80	117.10	25.18	150.00	28.10	3.14
Non-aged 2% CFF/PLA	58.65	107.95	21.70	154.65	25.80	4.50
Aged 2% CFF/PLA	67.52	109.10	20.84	155.07	27.03	6.79
Non-aged 5% CFF/PLA	57.65	106.35	22.10	155.75	25.40	3.74
Aged 5% CFF/PLA	67.79	108.75	25.25	155.49	29.65	4.98
Non-aged 10% CFF/PLA	60.45	109.85	23.20	155.15	25.31	2.52
Aged 10% CFF/PLA	67.96	109.78	21.94	155.66	27.05	6.11

term ageing process; thus, they increase the total degree of crystallinity [35, 84, 94, 95]. The increase in crystallinity justifies the decrease in thermal stability. The small shoulders seen in the DSC curve of aged 10% CFF/PLA sample (Fig. 9) demonstrates the presence of new crystallites produced by the chain scission process, which leads to shorter molecular chains [94, 96]. It is also expected that yield and fracture stresses, and elastic and storage modules of CFF/PLA biocomposite samples to decrease with increasing degree of crystallinity [94, 97, 98]. In addition, it is obvious from the DSC curves that all the non-aged CFF/PLA biocomposite samples show a double endothermic melt peak. This behaviour has been associated with the melt recrystallization mechanism; the less perfect crystals in this region show melting at lower temperatures, and they reorganize as the heating process continues in stable crystals [94, 99].

Morphological analyses

The thermal characterisation results reveal that the crystallization behaviour is not similar for PLA and CFF/PLA composites. Comparing the ΔH_m and X_c values of the non-aged and aged PLA, it is seen that ΔH_m and X_c values decrease with the effect of the long-term ageing process. This decrease may be due to an

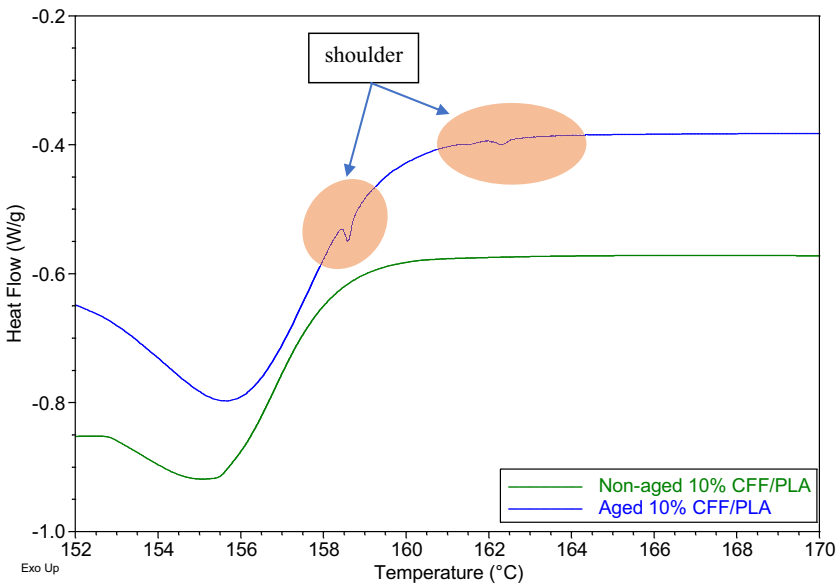

Fig. 9 DSC curves for melting heat of 10% CFF/PLA biocomposite samples

application that can affect the polymeric structure of the material, such as the ageing process, which prevents polymeric molecular chains to diffuse and migrate to the surface of the growing face of the polymer [35, 79, 84, 93, 100–102]. The reason that the ageing process can prevent the diffusion and migration of the polymeric molecular chains and prevent the rearrangement of the polymeric molecular chains is the impurities formed on the PLA surface [35, 100]. These impurities are formed by the ageing effect on the PLA surface as can be seen in Fig. 10. The aged PLA morphology demonstrates more broken and a rougher surface than the non-aged PLA.

SEM micrographs of fracture surface of non-aged and aged CFF/PLA biocomposite samples are given in Fig. 11. When micrographs of samples with the same CFF mass ratio are compared to each other, it is seen that the aged samples have more microvoids, cavities and gaps between fibre and matrix. As a result of the long-term ageing process, it is seen that cavities and microvoids on the fracture surfaces of CFF/PLA biocomposite samples increase, and the interfacial bonding success between the CFF and matrix material PLA decreases. One of the parameters that express the quality of the interfacial bonding between the fibres and the matrix is the gaps formed between the fibre and the matrix. As the numbers of gaps increases, the quality of the interfacial bonding between the fibres and the matrix decreases [103]. In this context, when micrographs of aged and non-aged samples are examined, more gaps are observed between the fibres and matrix in the aged samples. This indicates that the interfacial bonding between the fibres and the matrix of aged samples is weaker.

The strong interfacial bonding between the matrix and the reinforcing element, and the morphological stability are considered among the factors that cause the high thermal stability of the composite [89, 104–107]. As can be seen in the Fig. 11, the ageing process has an impact on the surface morphology of the biocomposite sample; thus, the presence of microvoids and cavities on the surface led to morphological instability. In addition, the interfacial bonding failure between PLA and CFF with the effect of the ageing process is one of the reasons that cause thermal stability to decline.

Conclusions

In this study, the effect of long term natural atmospheric ageing process on thermal properties of CFF/PLA biocomposite samples having different CFF mass concentration ratios were investigated. With the findings obtained from the experimental study, the following conclusions can be drawn;

- According to the results of TGA, the residual mass ratio of PLA does not change with the effect of ageing, whereas the ageing process increases the mass loss of CFF/PLA samples as the CFF mass ratio decreases. Accordingly, the reduction in residual mass ratios is 2.79% for 2% CFF/PLA, 0.95% for 5% CFF/PLA, and 0.76% for 10% CFF/PLA.
- According to DTG curves, decreases in decomposition peaks of CFF/PLA biocomposite samples are observed with the effect of ageing process. The decomposition peak of PLA decreases by 2.70% to 348.03 °C, that of the CFF decreases by 0.99% to 326.53 °C, that of 2% CFF/PLA decreases by 3.79% to 338.07 °C, that of 5% CFF/PLA decreases by 3.77% to 335.48 °C, and that of 10% CFF/PLA decreases by 1.92% to 339.05 °C.
- By overlapping the DTA and TGA curves, it is seen that the thermal stability of the samples decreases with the effect of the ageing process. Accordingly, T_{onset} of the

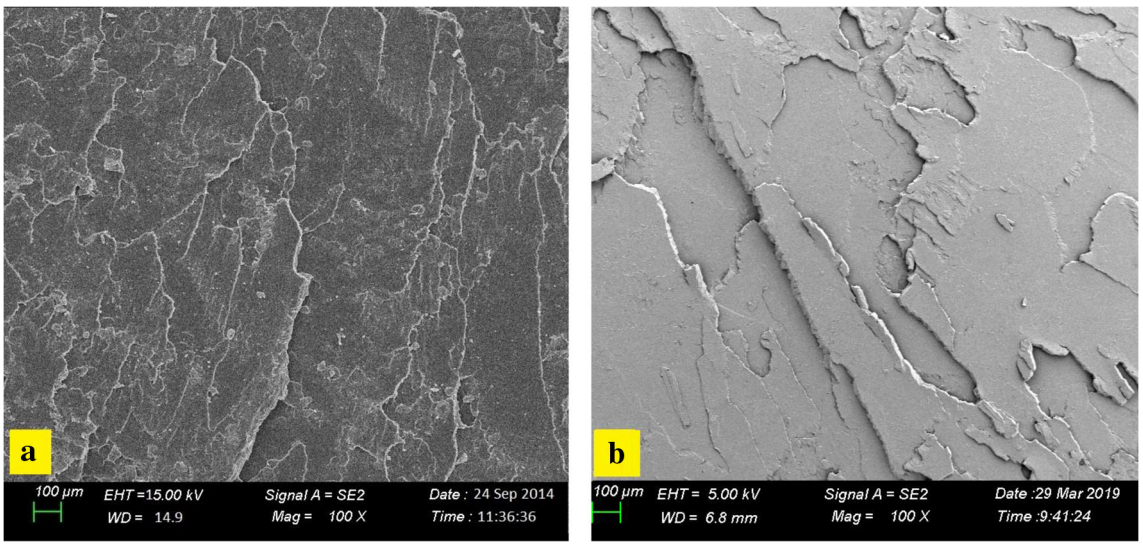

Fig. 10 SEM micrographs of (**a**) non-aged and (**b**) aged PLA samples

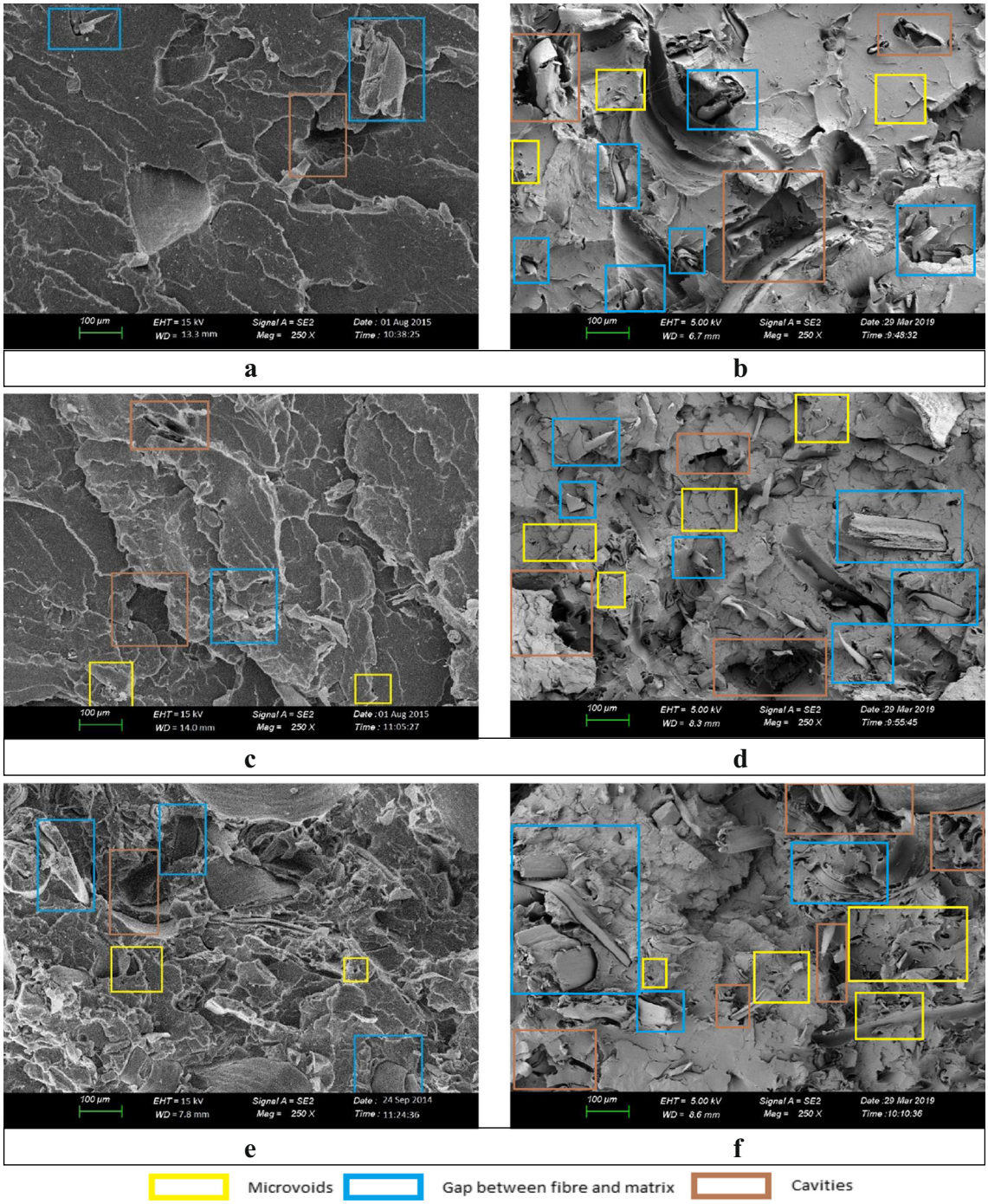

Fig. 11 Fracture morphology of non-aged and aged CFF/PLA biocomposite samples (**a** and **b**) 2%, (**c** and **d**) 5%, (**e** and **f**) 10%. The left panel shows the non-aged biocomposite samples and the right panel shows the aged biocomposite samples

CFF decreases by 0.51% to 231.57 °C, that of PLA decreases by 0.59% to 336.43 °C, that of 2% CFF/PLA decreases by 1.35% to 315.30 °C, that of 5% CFF/PLA decreases by 2.31% to 308.40 °C and that of 10% CFF/PLA decreases by 0.14% to 315.66 °C.

- According to the DSC analysis results, increases in the X_c of the aged CFF/PLA biocomposite samples are noticed. This increase, which associated with the lamella thickening phenomenon, is 6.79% for 2% CFF/PLA, 4.98% for 5% CFF/PLA and 6.11% for 10% CFF/PLA.

The results contained herein may be useful in understanding the ageing mechanism of biocomposite materials. Moreover, the results can be used to determine the critical parameters that should be considered to ensure long-term performance of these composites.

References

1. Hassan MM, Koyama K (2020) Thermomechanical and viscoelastic properties of green composites of PLA using chitin micro-particles as fillers. J Polym Res 27. https://doi.org/10.1007/s10965-019-1991-2
2. Thomas S, Kuruvilla J, Malhotra SK et al (2012) Polymer composites. Wiley-VCH
3. Varley D, Yousaf S, Youseffi M, Mozafari M (2019) Fiber-reinforced composites. Adv dent biomater 301–315. https://doi.org/10.1016/B978-0-08-102476-8.00013-X
4. Keck S, Fulland M (2016) Effect of fibre volume fraction and fibre direction on crack paths in flax fibre-reinforced composites. Eng Fract Mech 167:201–209. https://doi.org/10.1016/j.engfracmech.2016.03.037
5. Peças P, Carvalho H, Salman H, Leite M (2018) Natural fibre composites and their applications: a review. J Compos Sci 2:66. https://doi.org/10.3390/jcs2040066
6. Vroman I, Tighzert L (2009) Biodegradable polymers. Materials (Basel) 2:307–344
7. Shimao M (2001) Biodegradation of plastics. Curr Opin Biotechnol 12:242–247
8. Shah AA, Hasan F, Hameed A, Ahmed S (2008) Biological degradation of plastics: a comprehensive review. Biotechnol Adv 26:246–265
9. Murthy N, Wilson S, Sy JC (2012) Biodegradation of polymers. In: polymer science: a comprehensive reference, 10 volume set. Elsevier, pp 547–560
10. Yin GZ, Yang XM (2020) Biodegradable polymers: a cure for the planet, but a long way to go. J Polym Res 27
11. Papageorgiou GZ (2018) Thinking green: sustainable polymers from renewable resources. Polymers (Basel) 10
12. Schneiderman DK, Hillmyer MA (2017) 50th anniversary perspective: there is a great future in sustainable polymers. Macromolecules 50:3733–3749. https://doi.org/10.1021/acs.macromol.7b00293
13. Mitra BC (2014) Environment friendly composite materials: biocomposites and green composites. Def Sci J 64:244–261. https://doi.org/10.14429/dsj.64.7323
14. Mohanty AK, Misra M, Drzal LT (2005) Natural fibers, biopolymers, and biocomposites. CRC Press
15. Dicker MPM, Duckworth PF, Baker AB, Francois G, Hazzard MK, Weaver PM (2014) Green composites: a review of material attributes and complementary applications. Compos Part A Appl Sci Manuf 56:280–289
16. Zhu Y, Romain C, Williams CK (2016) Sustainable polymers from renewable resources. Nature 540:354–362
17. Auras R, Harte B, Selke S (2004) An overview of polylactides as packaging materials. Macromol Biosci 4:835–864
18. Graupner N, Herrmann AS, Müssig J (2009) Natural and man-made cellulose fibre-reinforced poly(lactic acid) (PLA) composites: an overview about mechanical characteristics and application areas. Compos Part A Appl Sci Manuf 40:810–821. https://doi.org/10.1016/j.compositesa.2009.04.003
19. Inkinen S, Hakkarainen M, Albertsson A-C, Södergård A (2011) From lactic acid to poly(lactic acid) (PLA): characterization and analysis of PLA and its precursors. Biomacromolecules 12:523–532. https://doi.org/10.1021/bm101302t
20. Gupta B, Revagade N, Hilborn J (2007) Poly(lactic acid) fiber: an overview. Prog Polym Sci 32:455–482
21. Abdel-Rahman MA, Tashiro Y, Sonomoto K (2013) Recent advances in lactic acid production by microbial fermentation processes. Biotechnol Adv 31:877–902
22. Chafran LS, Campos JMC, Santos JS, Sales MJA, Dias SCL, Dias JA (2016) Synthesis of poly(lactic acid) by heterogeneous acid catalysis from d,l-lactic acid. J Polym Res 23:107. https://doi.org/10.1007/s10965-016-0976-7
23. S SK, Hiremath SS (2019) Natural Fiber reinforced composites in the context of biodegradability: a review. In: Reference Module in Materials Science and Materials Engineering. Elsevier
24. Faruk O, Bledzki AK, Fink HP, Sain M (2012) Biocomposites reinforced with natural fibers: 2000-2010. Prog Polym Sci 37:1552–1596
25. Mukherjee T, Kao N (2011) PLA based biopolymer reinforced with natural fibre: a review. J Polym Environ 19:714–725. https://doi.org/10.1007/s10924-011-0320-6
26. Yu T, Ren J, Li S, Yuan H, Li Y (2010) Effect of fiber surface-treatments on the properties of poly(lactic acid)/ramie composites. Compos Part A Appl Sci Manuf 41:499–505. https://doi.org/10.1016/j.compositesa.2009.12.006
27. Graupner N, Müssig J (2011) A comparison of the mechanical characteristics of kenaf and lyocell fibre reinforced poly(lactic acid) (PLA) and poly(3-hydroxybutyrate) (PHB) composites. Compos Part A Appl Sci Manuf 42:2010–2019. https://doi.org/10.1016/j.compositesa.2011.09.007
28. Bledzki AK, Jaszkiewicz A, Scherzer D (2009) Mechanical properties of PLA composites with man-made cellulose and abaca fibres. Compos Part A Appl Sci Manuf 40:404–412. https://doi.org/10.1016/j.compositesa.2009.01.002
29. Shih YF, Huang CC (2011) Polylactic acid (PLA)/banana fiber (BF) biodegradable green composites. J Polym Res 18:2335–2340. https://doi.org/10.1007/s10965-011-9646-y
30. Noorunnisa Khanam P, Abdul Khalil HPS, Ramachandra Reddy G, Venkata Naidu S (2011) Tensile, flexural and chemical resistance properties of sisal fibre reinforced polymer composites: effect of fibre surface treatment. J Polym Environ 19:115–119. https://doi.org/10.1007/s10924-010-0219-7
31. Sutivisedsak N, Cheng HN, Dowd MK, Selling GW, Biswas A (2012) Evaluation of cotton byproducts as fillers for poly(lactic acid) and low density polyethylene. Ind Crop Prod 36:127–134. https://doi.org/10.1016/j.indcrop.2011.08.016
32. Dauda BMD, Kolawole EG (2003) Processibility of Nigerian kapok fibre. Indian J Fibre Text Res 28:147–149
33. Fan Z, Hu J, Wang J (2012) Biological nitrate removal using wheat straw and PLA as substrate. Environ Technol (United Kingdom) 33:2369–2374. https://doi.org/10.1080/09593330.2012.669411
34. Okubo K, Fujii T, Thostenson ET (2009) Multi-scale hybrid biocomposite: processing and mechanical characterization of bamboo fiber reinforced PLA with microfibrillated cellulose. Compos Part A Appl Sci Manuf 40:469–475. https://doi.org/10.1016/j.compositesa.2009.01.012
35. Luo H, Xiong G, Ma C, Chang P, Yao F, Zhu Y, Zhang C, Wan Y (2014) Mechanical and thermo-mechanical behaviors of sizing-treated corn fiber/polylactide composites. Polym Test 39:45–52. https://doi.org/10.1016/j.polymertesting.2014.07.014
36. Maringa M, Mutuli S, Kavishe F (2011) An investigation of the mechanical properties of sisal fibre. Loofah Matt and their Composites with Epoxy Resin J Agric Sci Technol 1. https://doi.org/10.4314/jagst.v1i1.31698
37. Prusek J, Boruvka M, Lenfeld P (2018) Natural aerobic degradation of Polylactic acid (composites) with natural Fiber additives. Mater Sci Forum 919:167–174. https://doi.org/10.4028/www.scientific.net/msf.919.167
38. Sun RC, Sun XF (2002) Structural and thermal characterization of acetylated rice, wheat, rye, and barley straws and poplar wood fibre. Ind Crop Prod 16:225–235. https://doi.org/10.1016/S0926-6690(02)00050-X
39. Smitthipong W, Tantatherdtam R, Chollakup R (2015) Effect of pineapple leaf fiber-reinforced thermoplastic starch/poly(lactic acid) green composite: mechanical, viscosity, and water resistance

properties. J Thermoplast Compos Mater 28:717–729. https://doi.org/10.1177/0892705713489701
40. Li Y, Shen YO (2014) The use of sisal and henequen fibres as reinforcements in composites. Biofiber Reinforcements in Composite Materials. Elsevier Inc., In, pp 165–210
41. Nassiopoulos E, Njuguna J (2015) Thermo-mechanical performance of poly(lactic acid)/flax fibre-reinforced biocomposites. Mater Des 66: 473–485. https://doi.org/10.1016/j.matdes.2014.07.051
42. Song YS, Lee JT, Ji DS, Kim MW, Lee SH, Youn JR (2012) Viscoelastic and thermal behavior of woven hemp fiber reinforced poly(lactic acid) composites. Compos Part B Eng 43:856–860. https://doi.org/10.1016/j.compositesb.2011.10.021
43. Anand P, Rajesh D, Senthil Kumar M, Saran Raj I (2018). Investigations on the performances of treated jute/Kenaf hybrid natural fiber reinforced epoxy composite J Polym Res:25. https://doi.org/10.1007/s10965-018-1494-6
44. Dong Y, Ghataura A, Takagi H, Haroosh HJ, Nakagaito AN, Lau KT (2014) Polylactic acid (PLA) biocomposites reinforced with coir fibres: evaluation of mechanical performance and multifunctional properties. Compos Part A Appl Sci Manuf 63:76–84. https://doi.org/10.1016/j.compositesa.2014.04.003
45. Mamun AA, Heim HP, Beg DH, Kim TS, Ahmad SH (2013) PLA and PP composites with enzyme modified oil palm fibre: a comparative study. Compos Part A Appl Sci Manuf 53:160–167. https://doi.org/10.1016/j.compositesa.2013.06.010
46. Wu CS, Tsou CH (2019) Fabrication, characterization, and application of biocomposites from poly(lactic acid) with renewable rice husk as reinforcement. J Polym Res 26. https://doi.org/10.1007/s10965-019-1710-z
47. Hidalgo-Cordero JF, García-Navarro J (2018) Totora (Schoenoplectus californicus (C.a. Mey.) Soják) and its potential as a construction material. Ind. Crops Prod 112:467–480
48. Bard D, Yarwood J, Tylee B (1997) Asbestos fibre identification by Raman microspectroscopy. J Raman Spectrosc 28:803–809. 10.1002/(SICI)1097-4555(199710)28:10<803::AID-JRS151>3.0.CO;2-7
49. Croce A, Arrais A, Rinaudo C (2018) Raman micro-spectroscopy identifies carbonaceous particles lying on the surface of Crocidolite, Amosite, and Chrysotile fibers. Minerals 8:249. https://doi.org/10.3390/min8060249
50. Pollastri S, Perchiazzi N, Gigli L et al (2017) The crystal structure of mineral fibres. 2. Amosite and fibrous anthophyllite. Period di Mineral 86:55–65. https://doi.org/10.2451/2017PM693
51. Pollastri S, Perchiazzi N, Lezzerini M et al (2016) The crystal structure of mineral fibres. 1. Chrysotile. Period di Mineral 85: 249–259. https://doi.org/10.2451/2016PM655
52. Bloise A, Kusiorowski R, Gualtieri A (2018) The effect of grinding on Tremolite Asbestos and Anthophyllite Asbestos. Minerals 8:274. https://doi.org/10.3390/min8070274
53. Bolormaa B, Drean JY, Enkhtuya D (2007) A study of the diameter distribution and tensile property of horse tail hair. J Nat Fibers 4:1–11
54. Verma A, Singh VK (2016) Human hair: a biodegradable composite Fiber–a review. Int J Waste Resour 6. https://doi.org/10.4172/2252-5211.1000206
55. Dunmade I (2013) Mechanical properties of renewable materials : a study on alpaca fibre. Int J Enginnering Sci Invent 2:56–62
56. Bharath KN, Pasha M, Nizamuddin BA (2016) Characterization of natural fiber (sheep wool)-reinforced polymer-matrix composites at different operating conditions. J Ind Text 45:730–751. https://doi.org/10.1177/1528083714540698
57. Molins G, Álvarez MD, Garrido N, Macanás J, Carrillo F (2018) Environmental impact assessment of Polylactide(PLA)/chicken feathers biocomposite materials. J Polym Environ 26:873–884. https://doi.org/10.1007/s10924-017-0982-9
58. Srivatsav V, Ravishankar C, Ramakarishna M et al (2018) Mechanical and thermal properties of chicken feather reinforced epoxy composite. AIP Conference Proceedings. American Institute of Physics Inc., In
59. Reddy N, Yang Y (2007) Structure and properties of chicken feather barbs as natural protein fibers. J Polym Environ 15:81–87. https://doi.org/10.1007/s10924-007-0054-7
60. Bessa J, Souza J, Lopes JB et al (2017) Characterization of thermal and acoustic insulation of chicken feather reinforced composites. Procedia Engineering. Elsevier Ltd, In, pp 472–479
61. Zhan M, Wool RP, Xiao JQ (2011) Electrical properties of chicken feather fiber reinforced epoxy composites. Compos Part A Appl Sci Manuf 42:229–233. https://doi.org/10.1016/j.compositesa.2010.11.007
62. Özmen U, Baba BO (2017) Thermal characterization of chicken feather/PLA biocomposites. J Therm Anal Calorim 129:347–355. https://doi.org/10.1007/s10973-017-6188-5
63. Cheng S, Lau K tak, Liu T, et al (2009) Mechanical and thermal properties of chicken feather fiber/PLA green composites. Compos Part B Eng 40:650–654. https://doi.org/10.1016/j.compositesb.2009.04.011
64. Malloum A, El Mahi A, Idriss M (2019) The effects of water ageing on the tensile static and fatigue behaviors of greenpoxy–flax fiber composites. J Compos Mater 53:2927–2939. https://doi.org/10.1177/0021998319835596
65. Techawinyutham L, Siengchin S, Dangtungee R, Parameswaranpillai J (2019) Influence of accelerated weathering on the thermo-mechanical, antibacterial, and rheological properties of polylactic acid incorporated with porous silica-containing varying amount of capsicum oleoresin. Compos part B Eng 175. https://doi.org/10.1016/j.compositesb.2019.107108
66. Isadounene S, Hammiche D, Boukerrou A, Rodrigue D, Djidjelli H (2018) Accelerated ageing of alkali treated olive husk flour reinforced polylactic acid (pla) biocomposites: Physico-mechanical properties. Polym Polym Compos 26:223–232. https://doi.org/10.1177/096739111802600302
67. Lila MK, Shukla K, Komal UK, Singh I (2019) Accelerated thermal ageing behaviour of bagasse fibers reinforced poly (lactic acid) based biocomposites. Compos Part B Eng 156:121–127. https://doi.org/10.1016/j.compositesb.2018.08.068
68. Gil-Castell O, Badia JD, Kittikorn T, Strömberg E, Ek M, Karlsson S, Ribes-Greus A (2016) Impact of hydrothermal ageing on the thermal stability, morphology and viscoelastic performance of PLA/sisal biocomposites. Polym Degrad Stab 132:87–96. https://doi.org/10.1016/j.polymdegradstab.2016.03.038
69. Pickett JE, Coyle DJ (2013) Hydrolysis kinetics of condensation polymers under humidity aging conditions. Polym Degrad Stab 98: 1311–1320. https://doi.org/10.1016/j.polymdegradstab.2013.04.001
70. Yu L, Yan X, Fortin G (2018) Effects of weathering aging on mechanical and thermal properties of injection molded glass fiber reinforced polypropylene composites. J Polym Res 25:247. https://doi.org/10.1007/s10965-018-1642-z
71. Kotsilkova R, Angelova P, Batakliev T et al (2019) Study on aging and recover of poly (lactic) acid composite films with graphene and carbon nanotubes produced by solution blending and extrusion. Coatings 9. https://doi.org/10.3390/coatings9060355
72. Le Duigou A, Bourmaud A, Davies P, Baley C (2014) Long term immersion in natural seawater of flax/PLA biocomposite. Ocean Eng 90:140–148. https://doi.org/10.1016/j.oceaneng.2014.07.021
73. Araújo MC, Martins JP, Mirkhalaf SM et al (2014) Predicting the mechanical behavior of amorphous polymeric materials under strain through multi-scale simulation. Applied Surface Science. Elsevier B.V, In, pp 37–46
74. Mirkhalaf SM, Fagerström M (2019) The mechanical behavior of polylactic acid (PLA) films: fabrication, experiments and modelling. Mech Time-Dependent Mater. https://doi.org/10.1007/s11043-019-09429-w

75. Acioli-Moura R, Sun XS (2008) Thermal degradation and physical aging of poly(lactic acid) and its blends with starch. Polym Eng Sci 48:829–836. https://doi.org/10.1002/pen.21019
76. Baba BO, Özmen U (2017) Preparation and mechanical characterization of chicken feather/PLA composites. Polym Compos 38: 837–845. https://doi.org/10.1002/pc.23644
77. Aranberri I, Montes S, Azcune I, Rekondo A, Grande HJ (2017) Fully biodegradable biocomposites with high chicken feather content. Polymers (Basel) 9. https://doi.org/10.3390/polym9110593
78. Ohkita T, Lee SH (2006) Thermal degradation and biodegradability of poly (lactic acid)/corn starch biocomposites. J Appl Polym Sci 100:3009–3017. https://doi.org/10.1002/app.23425
79. Naveen J, Jawaid M, Zainudin ES, Sultan MTH, Yahaya R, Abdul Majid MS (2019) Thermal degradation and viscoelastic properties of Kevlar/Cocos nucifera sheath reinforced epoxy hybrid composites. Compos Struct 219:194–202. https://doi.org/10.1016/j.compstruct.2019.03.079
80. Gheith MH, Aziz MA, Ghori W, Saba N, Asim M, Jawaid M, Alothman OY (2019) Flexural, thermal and dynamic mechanical properties of date palm fibres reinforced epoxy composites. J Mater Res Technol 8:853–860. https://doi.org/10.1016/j.jmrt.2018.06.013
81. Siakeng R, Jawaid M, Ariffin H, Salit MS (2018) Effects of surface treatments on tensile, thermal and fibre-matrix bond strength of coir and pineapple leaf Fibres with poly lactic acid. J Bionic Eng 15:1035–1046. https://doi.org/10.1007/s42235-018-0091-z
82. Martínez-Hernández AL, Velasco-Santos C, De Icaza M, Castaño VM (2005) Microstructural characterisation of keratin fibres from chicken feathers. Int J Environ Pollut 23:162–178. https://doi.org/10.1504/ijep.2005.006858
83. Asim M, Jawaid M, Nasir M, Saba N (2018) Effect of fiber loadings and treatment on dynamic mechanical, thermal and flammability properties of pineapple leaf fiber and kenaf phenolic composites. J Renew Mater 6:383–393. https://doi.org/10.7569/JRM.2017.634162
84. T SMK, Yorseng K, N R, et al (2019) Mechanical and thermal properties of spent coffee bean filler/poly(3-hydroxybutyrate-co-3-hydroxyvalerate) biocomposites: effect of recycling. Process Saf Environ Prot 187–195. https://doi.org/10.1016/j.psep.2019.02.008, 124
85. Anbukarasi K, Kalaiselvam S (2015) Study of effect of fibre volume and dimension on mechanical, thermal, and water absorption behaviour of luffa reinforced epoxy composites. Mater Des 66: 321–330. https://doi.org/10.1016/j.matdes.2014.10.078
86. Yang Y, Haurie L, Wen J, Zhang S, Ollivier A, Wang DY (2019) Effect of oxidized wood flour as functional filler on the mechanical, thermal and flame-retardant properties of polylactide biocomposites. Ind Crop Prod 130:301–309. https://doi.org/10.1016/j.indcrop.2018.12.090
87. Fernandes EM, Correlo VM, Mano JF, Reis RL (2015) Cork-polymer biocomposites: mechanical, structural and thermal properties. Mater Des 82:282–289. https://doi.org/10.1016/j.matdes.2015.05.040
88. Akderya T, Çevik M (2018) Investigation of thermal-oil environmental ageing effect on mechanical and thermal behaviours of E-glass fibre/epoxy composites. J Polym Res 25. https://doi.org/10.1007/s10965-018-1615-2
89. Jia S, Yu D, Zhu Y et al (2017) Morphology, crystallization and thermal behaviors of PLA-based composites: wonderful effects of hybrid GO/PEG via dynamic impregnating. Polymers (Basel) 9. https://doi.org/10.3390/polym9100528
90. De Rosa IM, Iannoni A, Kenny JM et al (2011) Poly(lactic acid)/Phormium tenax composites: morphology and thermo-mechanical behavior. Polym Compos 32:1362–1368. https://doi.org/10.1002/pc.21159
91. Auras R, Lim LT, Selke SEM, Tsuji H (2010) Poly(lactic acid): synthesis, structures, properties, processing, and applications. John Wiley and Sons
92. Tokiwa Y, Calabia BP (2006) Biodegradability and biodegradation of poly(lactide). Appl Microbiol Biotechnol 72:244–251
93. Jawaid M, Abdul Khalil HPS, Hassan A, Dungani R, Hadiyane A (2013) Effect of jute fibre loading on tensile and dynamic mechanical properties of oil palm epoxy composites. Compos Part B Eng 45:619–624. https://doi.org/10.1016/j.compositesb.2012.04.068
94. Fouad H (2010) Effect of long-term natural aging on the thermal, mechanical, and viscoelastic behavior of biomedical grade of ultra high molecular weight polyethylene. J Appl Polym Sci 118:17–24. https://doi.org/10.1002/app.32290
95. Şanlı S, Durmus A, Ercan N (2012) Effect of nucleating agent on the nonisothermal crystallization kinetics of glass fiber- and mineral-filled polyamide-6 composites. J Appl Polym Sci 125: E268–E281. https://doi.org/10.1002/app.36231
96. Di Lorenzo ML, Sajkiewicz P, La Pietra P, Gradys A (2006) Irregularly shaped DSC exotherms in the analysis of polymer crystallization. Polym Bull 57:713–721. https://doi.org/10.1007/s00289-006-0621-4
97. Askadskii A, Popova M, Matseevich T, Afanasyev E (2014) The influence of the degree of crystallinity on the elasticity modulus of polymers. Advanced Materials Research, In, pp 640–643
98. Gofman IV, Yudin VE, Orell O, Vuorinen J, Grigoriev AY, Svetlichnyi VM (2013) Influence of the degree of crystallinity on the mechanical and tribological properties of high-performance thermoplastics over a wide range of temperatures: from room temperature up to 250°C. J Macromol Sci Part B Phys 52:1848–1860. https://doi.org/10.1080/00222348.2013.808932
99. Jiang N, Abe H (2015) Crystallization and mechanical behavior of covalent functionalized carbon nanotube/poly(3-hydroxybutyrate-co-3-hydroxyvalerate) nanocomposites. J Appl Polym Sci 132. https://doi.org/10.1002/app.42136
100. Pan P, Zhu B, Kai W, Serizawa S, Iji M, Inoue Y (2007) Crystallization behavior and mechanical properties of bio-based green composites based on poly(L-lactide) and kenaf fiber. J Appl Polym Sci 105:1511–1520. https://doi.org/10.1002/app.26407
101. Li X, Liu KL, Wang M, Wong SY, Tjiu WC, He CB, Goh SH, Li J (2009) Improving hydrophilicity, mechanical properties and biocompatibility of poly[(R)-3-hydroxybutyrate-co-(R)-3-hydroxyvalerate] through blending with poly[(R)-3-hydroxybutyrate]-alt-poly(ethylene oxide). Acta Biomater 5: 2002–2012. https://doi.org/10.1016/j.actbio.2009.01.035
102. Cheung HY, Lau KT, Tao XM, Hui D (2008) A potential material for tissue engineering: silkworm silk/PLA biocomposite. Compos Part B Eng 39:1026–1033. https://doi.org/10.1016/j.compositesb.2007.11.009
103. Pereira GC, Rzatki FD, Mazzaferro L, Forin DM, Barra GMO (2016) Mechanical and thermo-physical properties of short glass fiber reinforced polybutylene terephthalate upon aging in lubricant/refrigerant mixture. Mater Res 19:1310–1318. https://doi.org/10.1590/1980-5373-MR-2016-0339
104. J. Shesan O, C. Stephen A, G. Chioma A, et al (2019) Fiber-Matrix Relationship for Composites Preparation. In: Composites from Renewable and Sustainable Materials [Working Title]. IntechOpen
105. Wang L, He C, Fu J (2019) Physical, mechanical, and thermal behavior analyses of basalt fiber-reinforced composites. Int J Plast Technol 23:123–131. https://doi.org/10.1007/s12588-019-09244-5

106. Lee JJ, Nam I, Kim H (2017) Thermal stability and physical properties of epoxy composite reinforced with silane treated basalt fiber. Fibers Polym 18:140–147. https://doi.org/10.1007/s12221-017-6752-4
107. Chen ZC, Tamachi T, Kulkarni R, Chawla KK, Koopman M (2008) Interfacial reaction behavior and thermal stability of barium zirconate-coated alumina fiber/alumina matrix composites. J Eur Ceram Soc 28:1149–1160. https://doi.org/10.1016/j.jeurceramsoc.2007.09.048